Hydrodynamic Simulations of Non-thermal Pressure in Galaxy Clusters

Kaylea Nelson

Yale University

Cluster Masses and Cosmology

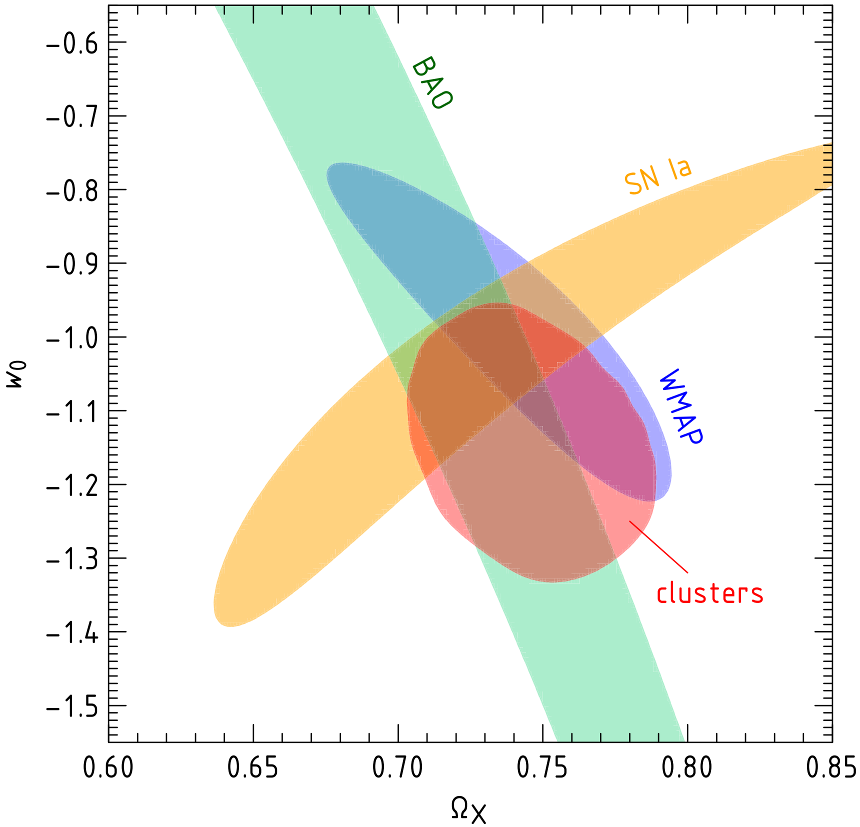

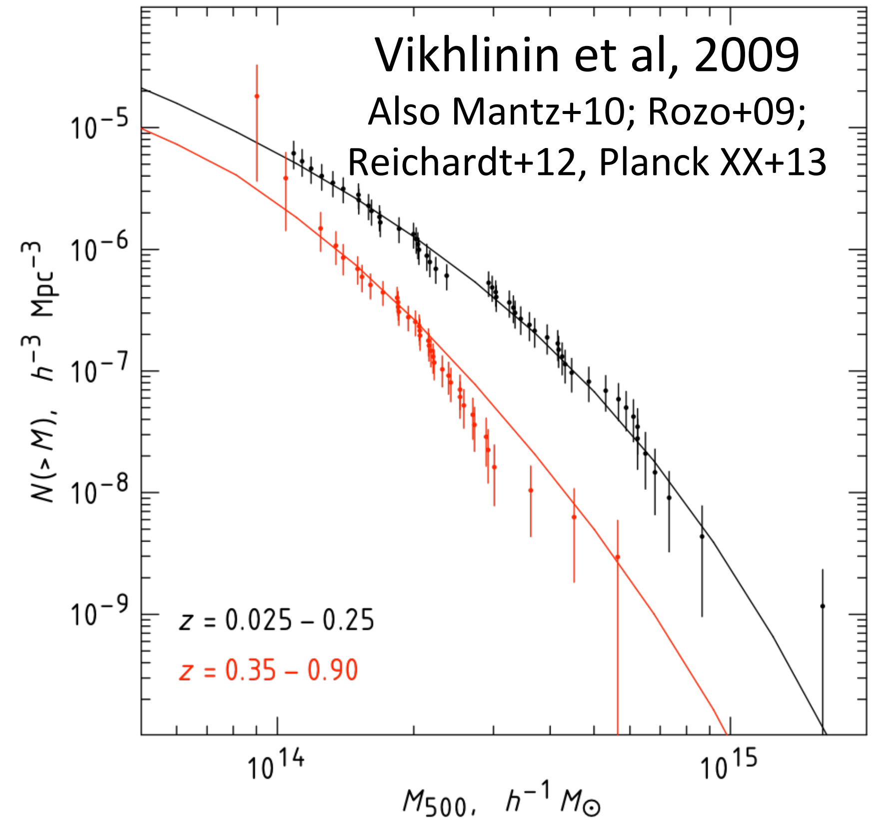

$\sigma_8 = 0.813(\Omega_M/0.25)^{-0.47} \pm 0.013$ (stat) $\pm$ **0.024 (sys)**

$w_0 = -0.991 \pm 0.045$ (stat) $\pm$ **0.039 (sys)**

$\Omega_{DE} = 0.740 \pm 0.012$

Hydrostatic Mass Estimate

Estimate the enclosed total mass (dark matter + gas + stars) within the sphere by assuming gas is in hydrostatic equilibrium with the gravitational potential

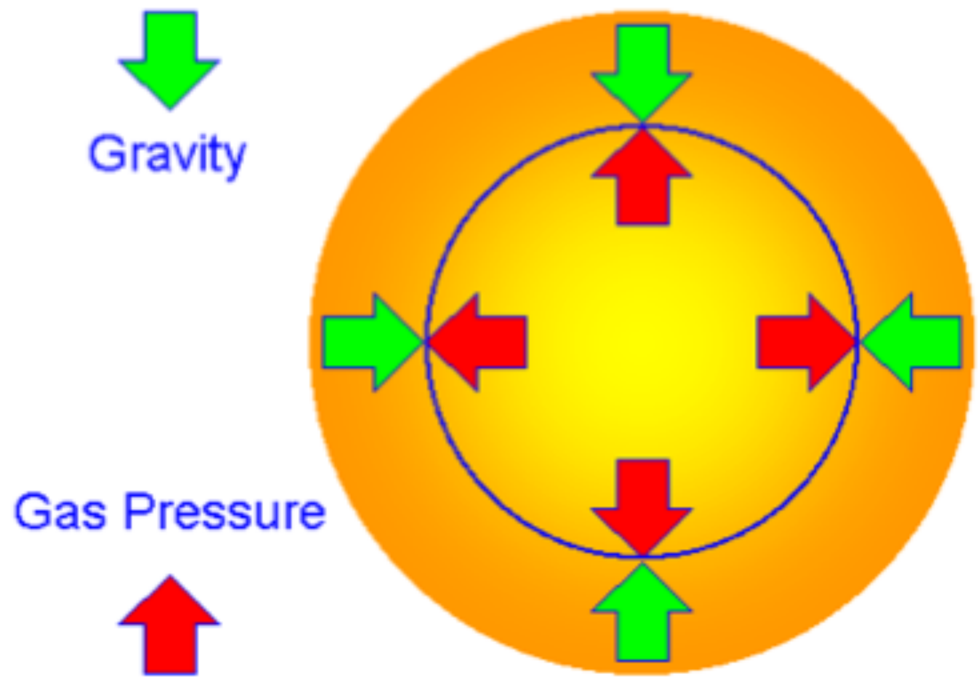

$$\frac{dP}{dr} = -\frac{GM(r)\rho(r)}{r^2} \qquad P = nk_BT$$

Determining Cluster Sizes

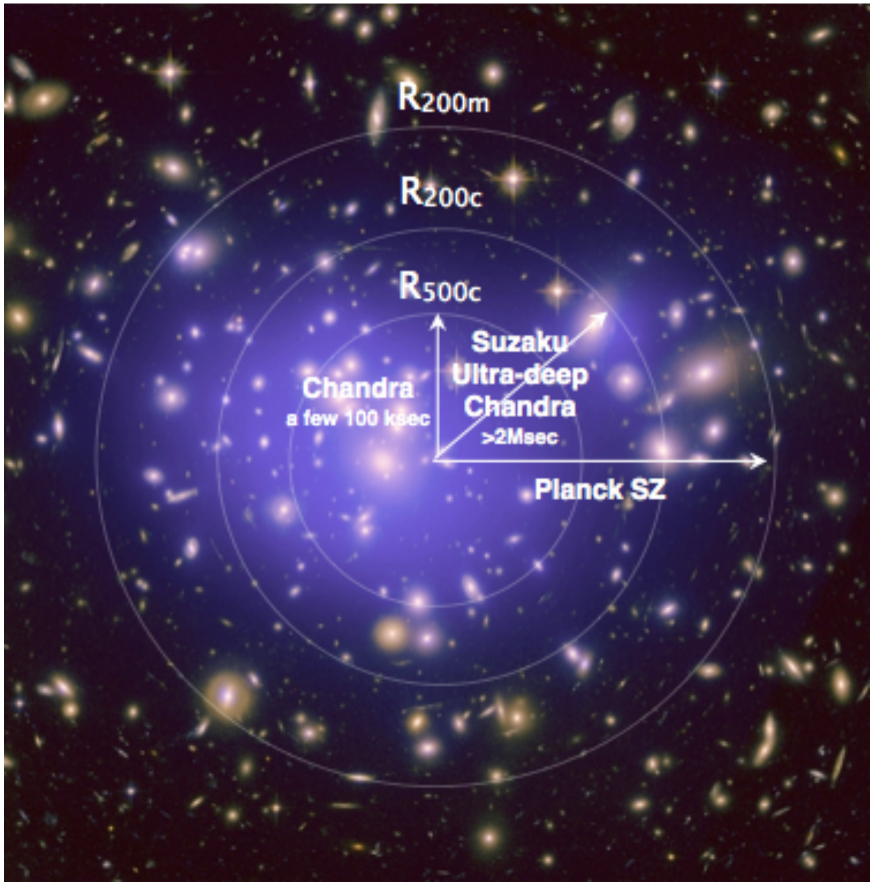

R_{500c}: R_{200c}: R_{200m} = 1: 1.4: 3

Unlike stars, galaxy clusters don't have a clear edge.

So, we need to define the enclosed mass (M_Δ) within a sphere of radius R_Δ, within which the average density is Δ times the **critical** or **mean** reference background mass density of the Universe.

$$M_\Delta \equiv \frac{4}{3}\pi R_\Delta^3(\Delta\rho_{crit})$$

Mass Reconstruction

By combining Gauss's Law for the gravitational field with the Euler equations that govern gas motions in simulations, the mass can be broken down into effective mass terms.

$$M = -\frac{1}{4\pi G}\int_{\partial V}\left(\frac{\partial u^i}{\partial t} + u^j\frac{\partial u^i}{\partial x^j} + \frac{1}{\rho}\frac{\partial P}{\partial x_i}\right) dS_i.$$

$$M(<r) = M_{\rm tot}(<r) = M_{\rm therm} + M_{\rm rand} + M_{\rm rot} + M_{\rm cross} + M_{\rm stream} + M_{\rm accel}, \quad (4)$$

where

$$M_{\rm therm} = \frac{-r^2}{G\langle\rho\rangle}\frac{\partial\langle P\rangle}{\partial r}, \quad (5)$$

$$M_{\rm rand} = \frac{-r^2}{G\langle\rho\rangle}\frac{\partial\langle\rho\rangle\sigma^2_{\rho,rr}}{\partial r} - \frac{r}{G}\left(2\sigma^2_{\rho,rr} - \sigma^2_{\rho,\theta\theta} - \sigma^2_{\rho,\phi\phi}\right), \quad (6)$$

$$M_{\rm rot} = \frac{r}{G}\left(\langle u_\theta\rangle^2_\rho + \langle u_\phi\rangle^2_\rho\right), \quad (7)$$

$$M_{\rm stream} = \frac{-r^2}{G}\left(\langle u_r\rangle_\rho\frac{\partial\langle u_r\rangle_\rho}{\partial r} + \frac{\langle u_\theta\rangle_\rho}{r}\frac{\partial\langle u_r\rangle_\rho}{\partial\theta} + \frac{\langle u_\phi\rangle_\rho}{r\sin\theta}\frac{\partial\langle u_r\rangle_\rho}{\partial\phi}\right), \quad (8)$$

$$M_{\rm cross} = \frac{-r^2}{G\langle\rho\rangle}\left(\frac{1}{r}\frac{\partial\langle\rho\rangle\sigma^2_{\rho,r\theta}}{\partial\theta} + \frac{1}{r\sin\theta}\frac{\partial\langle\rho\rangle\sigma^2_{\rho,r\phi}}{\partial\phi}\right) - \frac{r}{G}\left(\sigma^2_{\rho,r\theta}\cot\theta\right), \quad (9)$$

$$M_{\rm accel} = \frac{-r^2}{G}\frac{\partial\langle u_r\rangle_\rho}{\partial t}. \quad (10)$$

Lau, Nagai, Nelson 2013

Hydrostatic Mass Bias

- Mass commonly measured using hydrostatic mass estimate
- Underestimates mass by 10-30%
- Bias is due to additional non-thermal pressure from gas motions

$$M_{\rm tot} = M_{\rm therm} + M_{\rm vel} + M_{\rm accel}$$

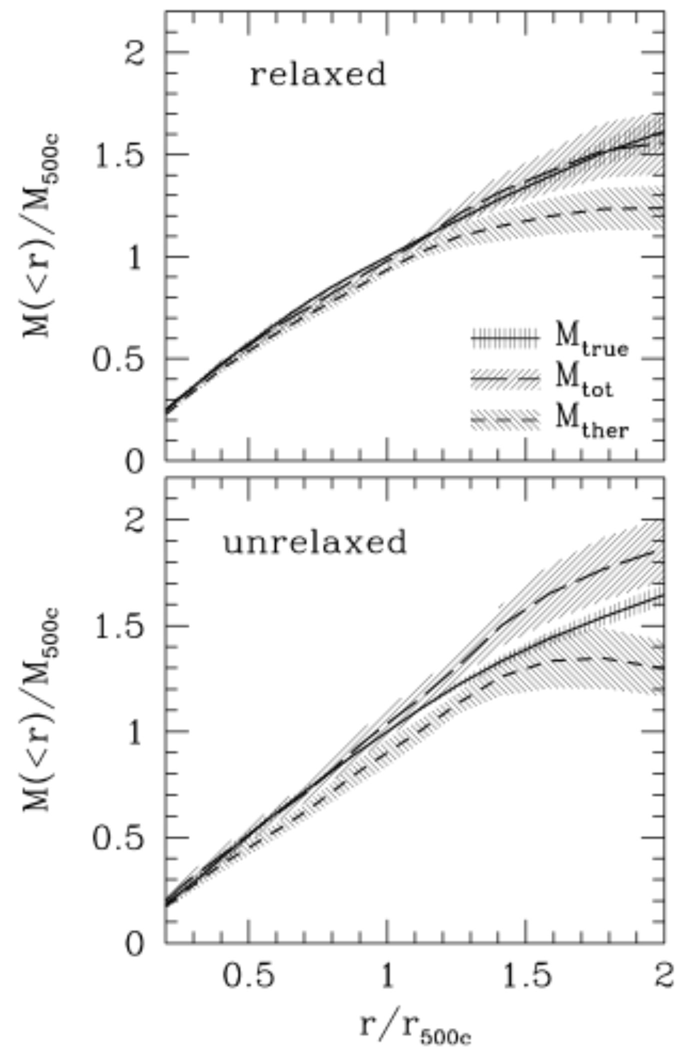

Lau, Kravtsov, Nagai, 2009

Omega 500 Simulation (Nelson et al. 2014)

N-body + Hydrodynamic Cosmological Simulation of Galaxy Clusters using ART

- Box Size: 500h^{-1} Mpc
- 512^3 root grid, effective 2048^3 resolution zoom-in regions
- Cosmologically representative, mass-limited sample of 65 clusters with $M_{500} = 3\text{x}10^{14} – 10^{15}\ h^{-1}M_\odot$
- Particle mass ≈ $10^9\ h^{-1}\ M_\odot$,
- Peak Resolution ≈ 3.8 h^{-1} kpc
- Focus on results from the non-radiative (NR) simulation, currently running with CSF+AGN
- Performed on the Yale Omega HPC cluster.

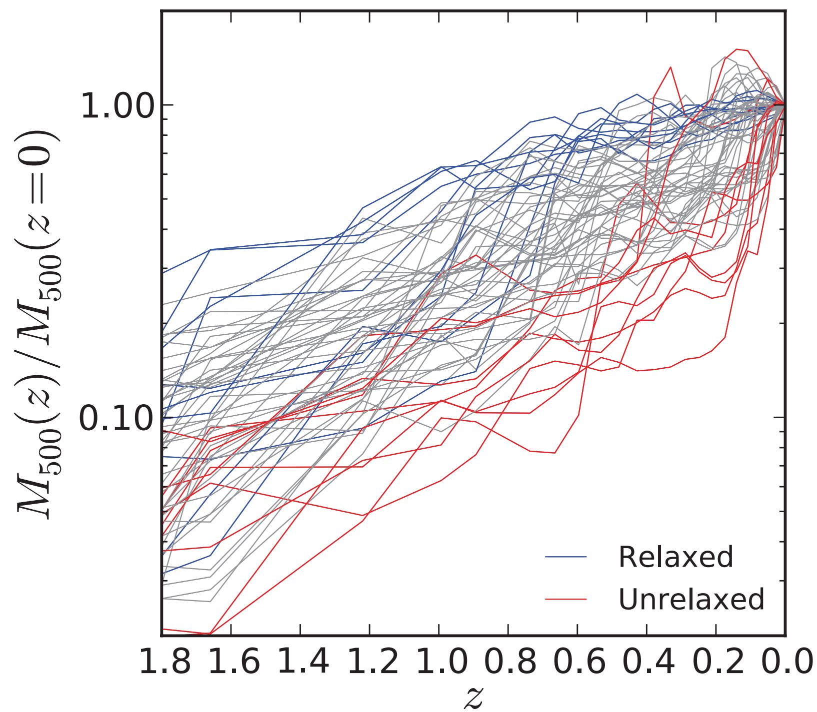

Merger Trees

Allows us to follow the evolution of cluster astrophysics as the cluster itself evolves

Merger Tree Code

- Maps the progenitors of halos through comparing bound particles between time steps
- Mergers are flagged by tracing all subhalos of the main progenitor back in time and out of the parent halo
- Mass ratio is measured when the two halos are separated by the sum of their virial radii

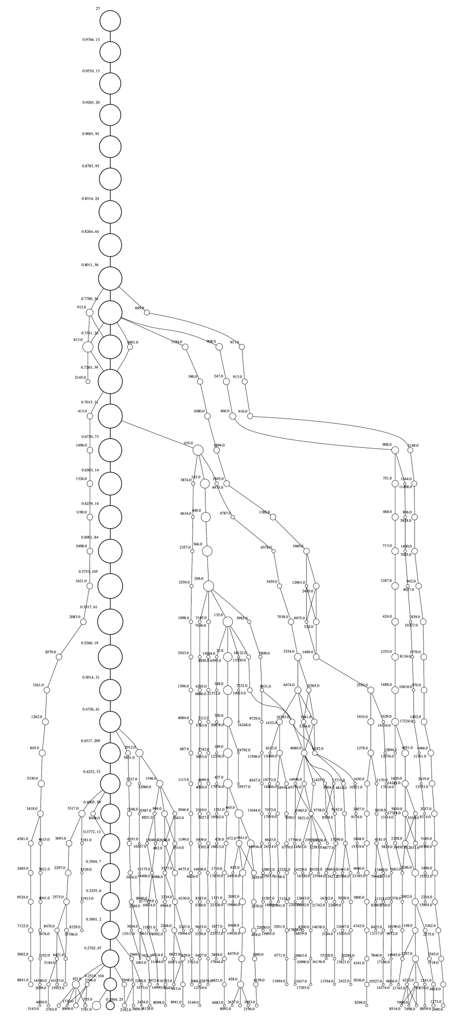

Evolution of Cluster during Merger

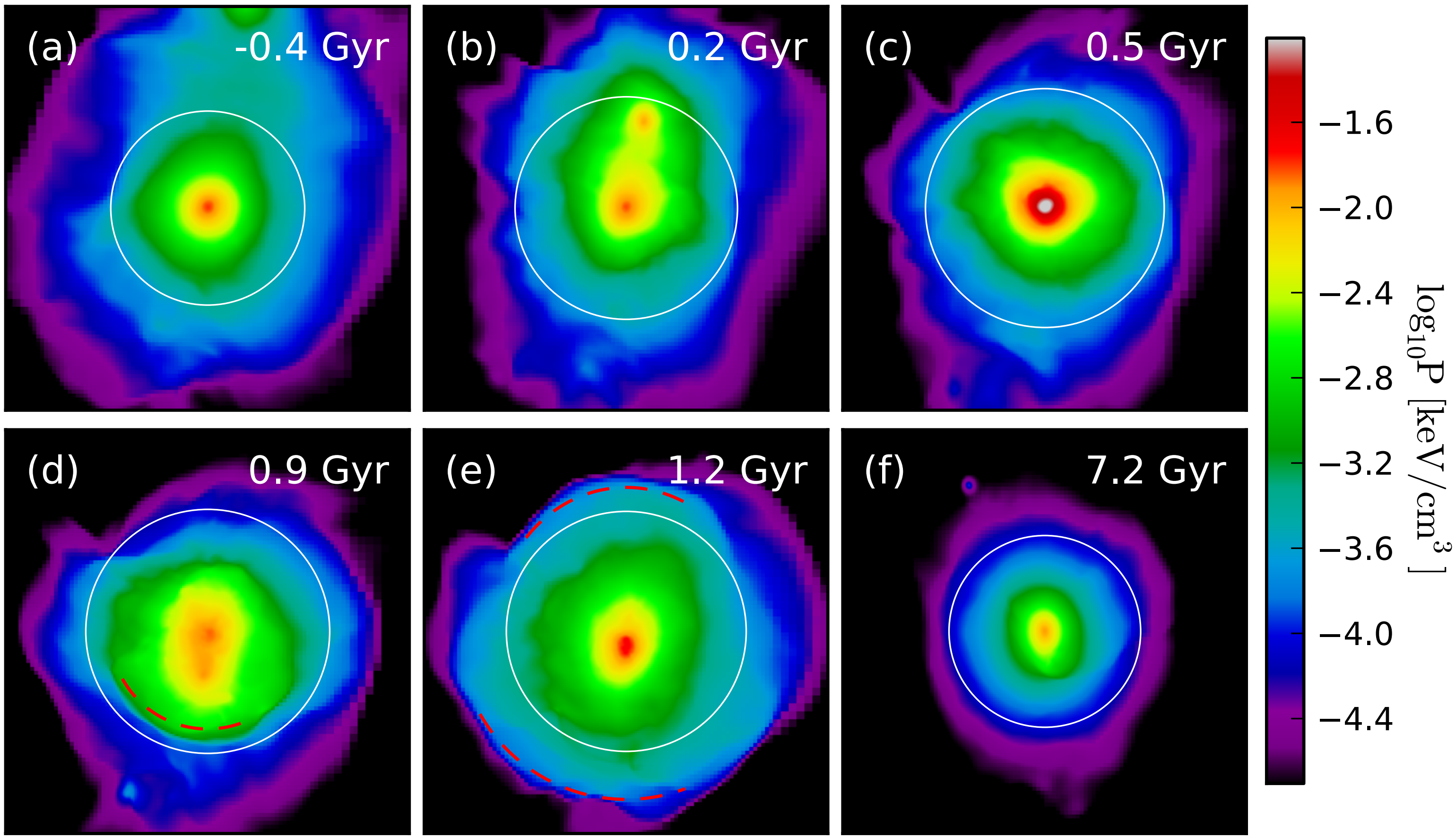

Nelson, Rudd, Shaw, Nagai, 2012, ApJ, 751, 121 (based on N07 sample)

Effect of Mergers on Mass Bias

- Increase in mass bias with radius
- Decrease in bias as clusters relax
- Only inner most regions reach zero bias even after 8 Gyr

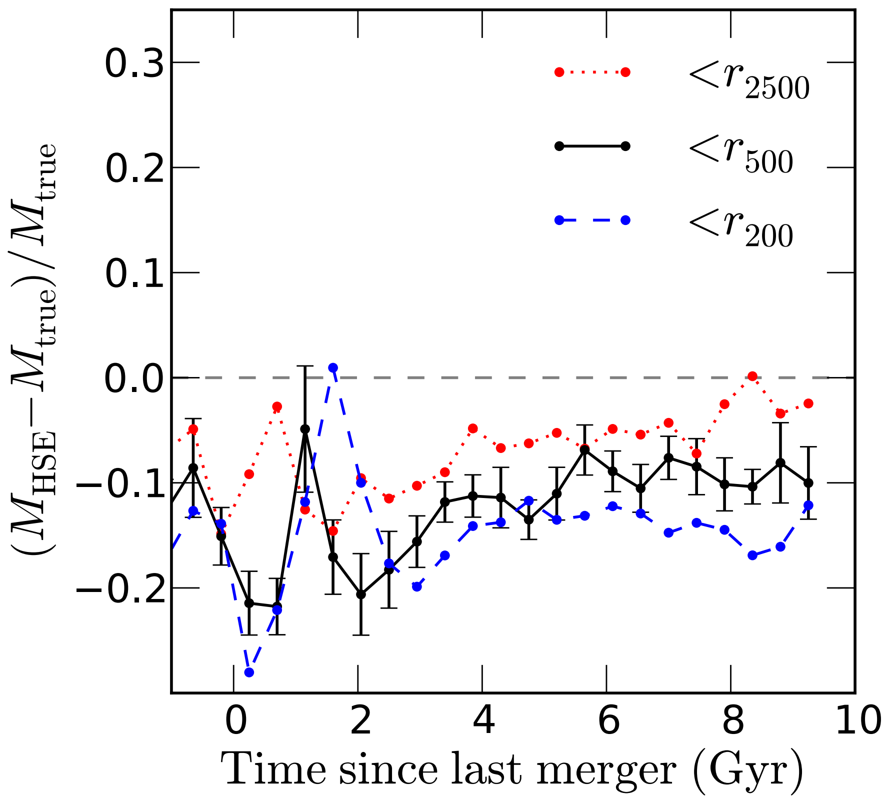

Nelson, Rudd, Shaw, Nagai, 2012, ApJ, 751, 12

Non-thermal Pressure Support

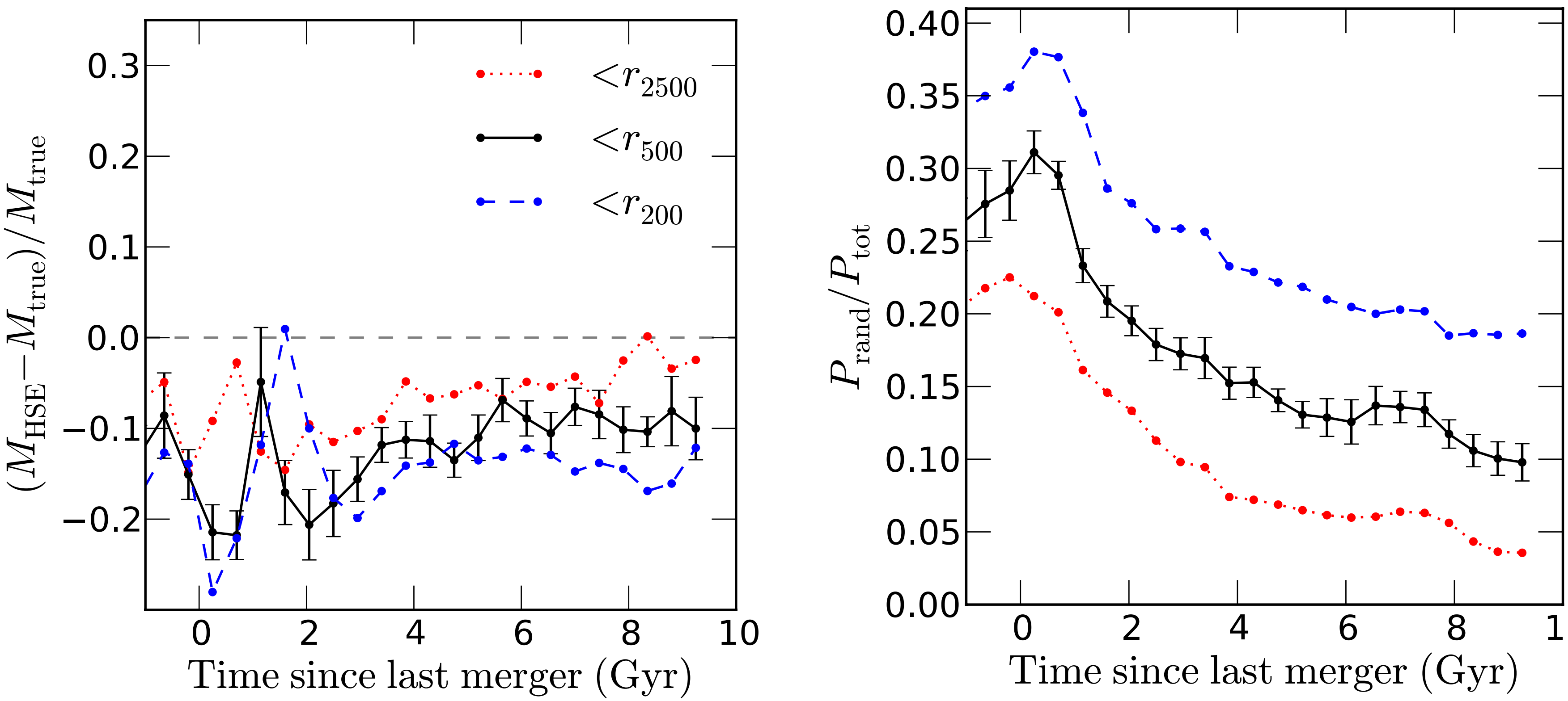

Non-thermal pressure due to random gas motions is one of the most dominant sources of systematic uncertainties in the HSE mass estimates of galaxy clusters (Nelson et al. 2012).

Non-thermal Pressure from Random Gas Motions

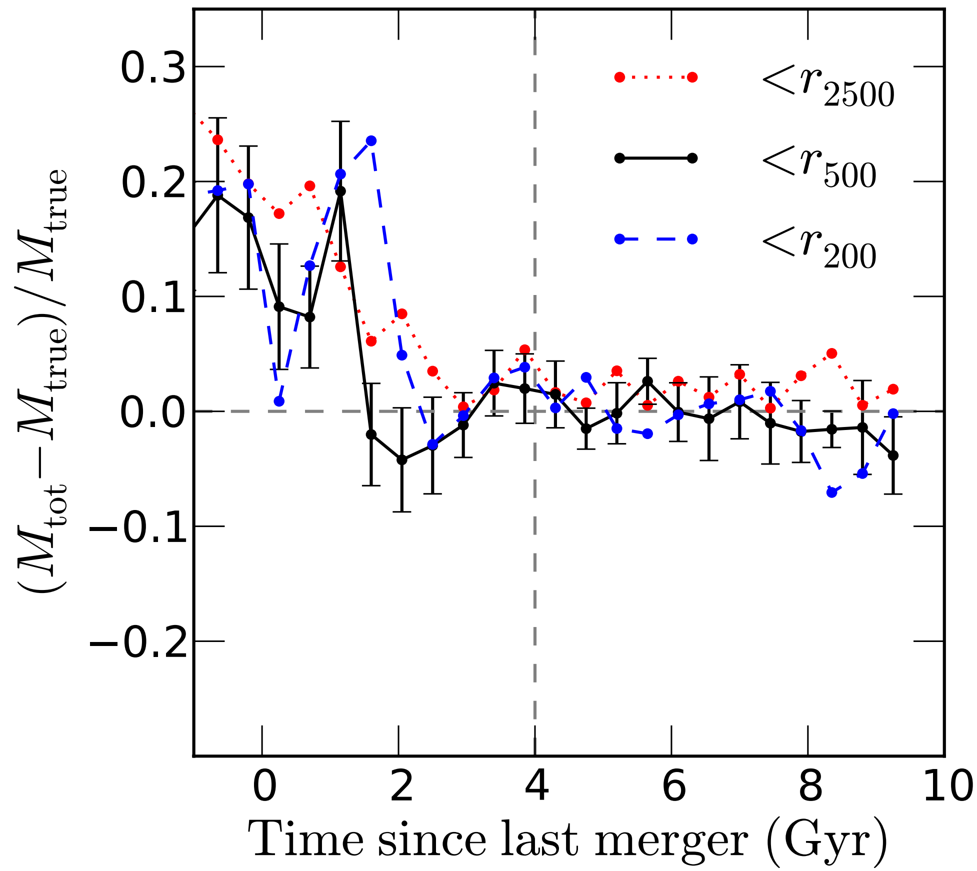

By accounting for non-thermal pressure from random gas motion, it is possible to recover the true mass for clusters with t_{merger} > 4 Gyr (Nelson et al. 2012).

Non-thermal Pressure in Y-M Relation

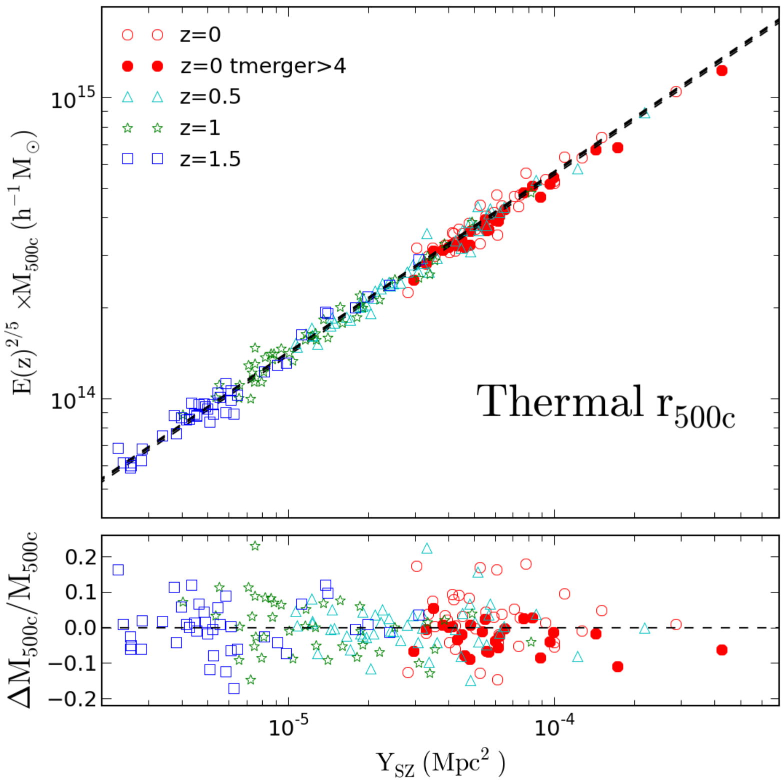

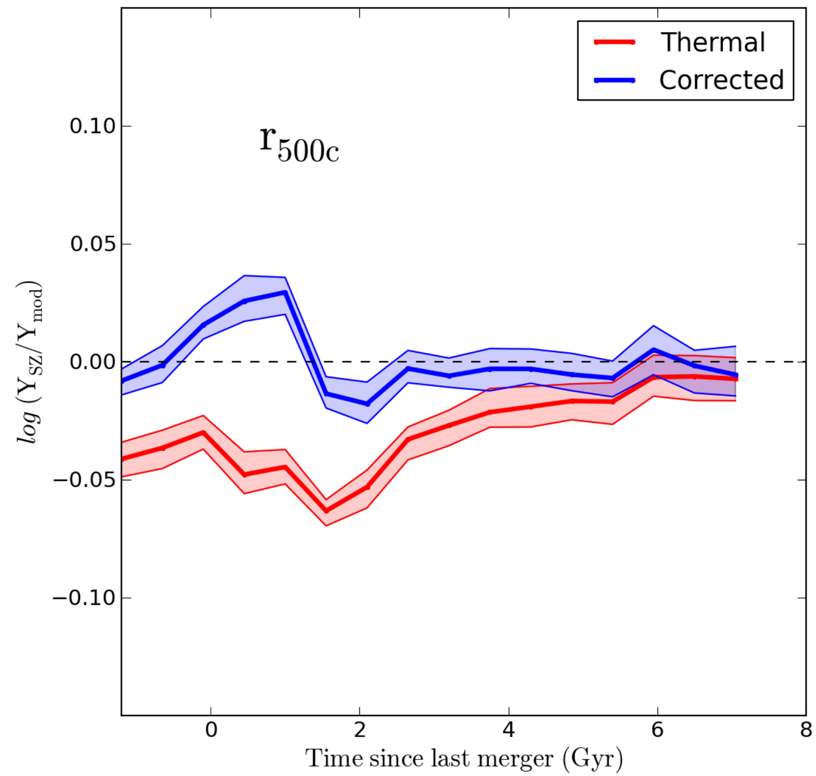

Dynamical state variations and non-thermal pressure are also responsible for scatter in the Y-M scaling relation.

Yu, Nelson, Nagai, Lau, in prep

Gas Velocity and Acceleration in a Relaxed Cluster

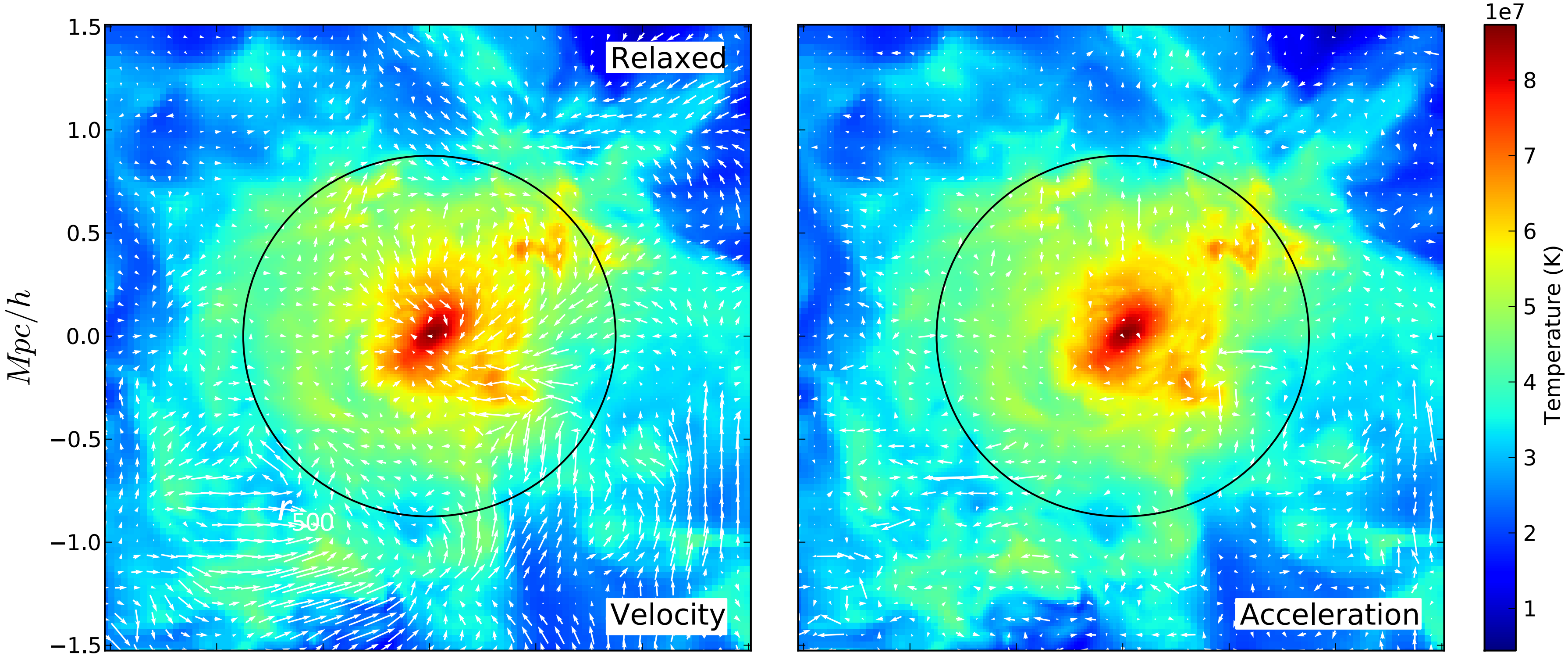

Gas is in "quasi"-hydrostatic equilibrium in the gravitational potential of galaxy clusters with non-negligible amount of gas motions, but little acceleration.

Nelson, Lau, Nagai, Rudd, Yu, 2014, ApJ, 782, 107

Gas Velocity and Acceleration in a Merging Cluster

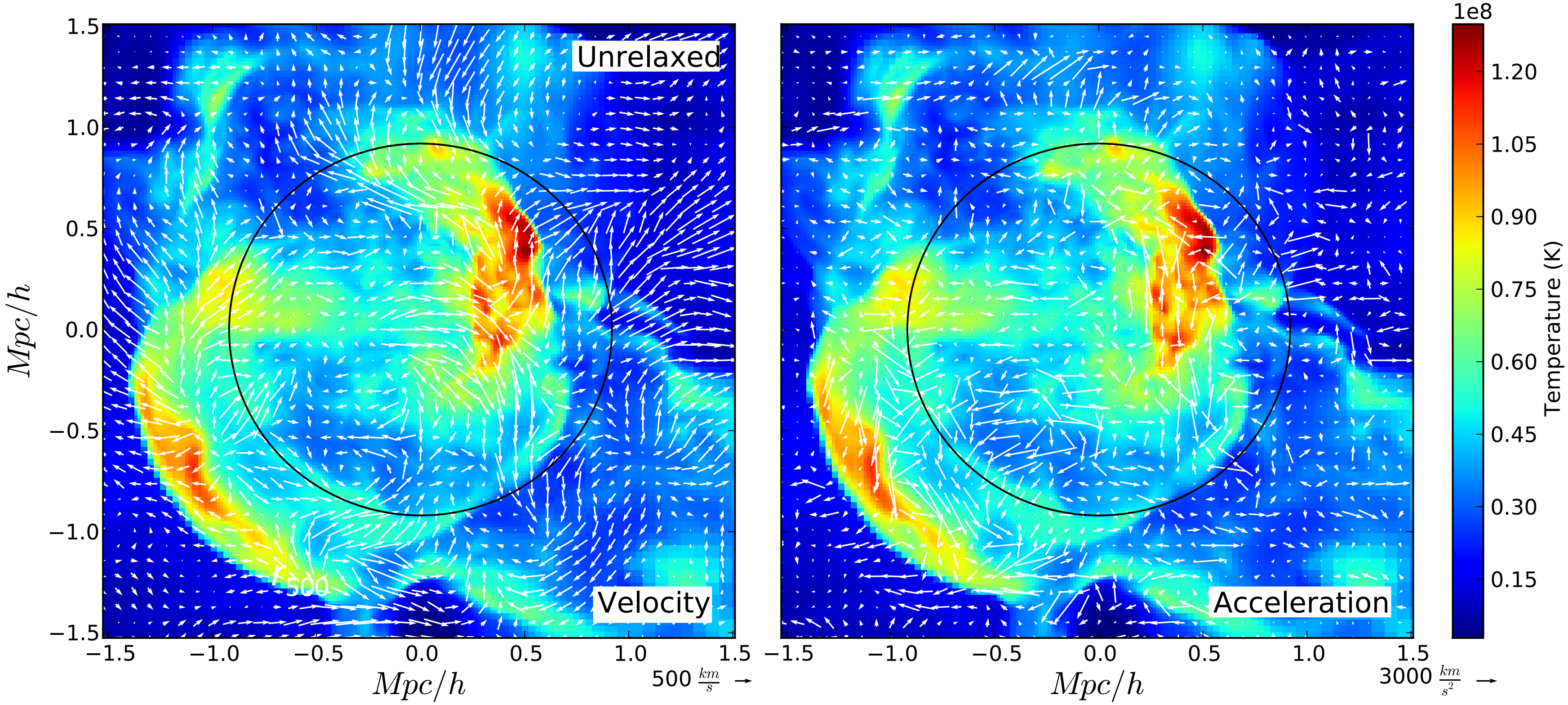

A major merger is a catastrophic event that generates significant gas motions, including gas acceleration due to merger shocks.

Nelson, Lau, Nagai, Rudd, Yu, 2014, ApJ, 782, 107

Full Non-thermal Pressure Support

By combining Gauss's Law for the gravitational field with the Euler equations that govern gas motions in simulations, the mass can be broken down into effective mass terms.

$$M = -\frac{1}{4\pi G}\int_{\partial V}\left(\frac{\partial u^i}{\partial t} + u^j\frac{\partial u^i}{\partial x^j} + \frac{1}{\rho}\frac{\partial P}{\partial x_i}\right) dS_i.$$

$$M(<r) = M_{\rm tot}(<r) = M_{\rm therm} + M_{\rm rand} + M_{\rm rot} + M_{\rm cross} + M_{\rm stream} + M_{\rm accel}, \quad (4)$$

where

$$M_{\rm therm} = \frac{-r^2}{G\langle\rho\rangle}\frac{\partial\langle P\rangle}{\partial r}, \quad (5)$$

$$M_{\rm rand} = \frac{-r^2}{G\langle\rho\rangle}\frac{\partial\langle\rho\rangle\sigma^2_{\rho,rr}}{\partial r} - \frac{r}{G}\left(2\sigma^2_{\rho,rr} - \sigma^2_{\rho,\theta\theta} - \sigma^2_{\rho,\phi\phi}\right), \quad (6)$$

$$M_{\rm rot} = \frac{r}{G}\left(\langle u_\theta\rangle^2_\rho + \langle u_\phi\rangle^2_\rho\right), \quad (7)$$

$$M_{\rm stream} = \frac{-r^2}{G}\left(\langle u_r\rangle_\rho\frac{\partial\langle u_r\rangle_\rho}{\partial r} + \frac{\langle u_\theta\rangle_\rho}{r}\frac{\partial\langle u_r\rangle_\rho}{\partial\theta} + \frac{\langle u_\phi\rangle_\rho}{r\sin\theta}\frac{\partial\langle u_r\rangle_\rho}{\partial\phi}\right), \quad (8)$$

$$M_{\rm cross} = \frac{-r^2}{G\langle\rho\rangle}\left(\frac{1}{r}\frac{\partial\langle\rho\rangle\sigma^2_{\rho,r\theta}}{\partial\theta} + \frac{1}{r\sin\theta}\frac{\partial\langle\rho\rangle\sigma^2_{\rho,r\phi}}{\partial\phi}\right) - \frac{r}{G}\left(\sigma^2_{\rho,r\theta}\cot\theta\right), \quad (9)$$

$$M_{\rm accel} = \frac{-r^2}{G}\frac{\partial\langle u_r\rangle_\rho}{\partial t}. \quad (10)$$

Lau, Nagai, Nelson 2013

HSE Mass Bias due to Gas Acceleration

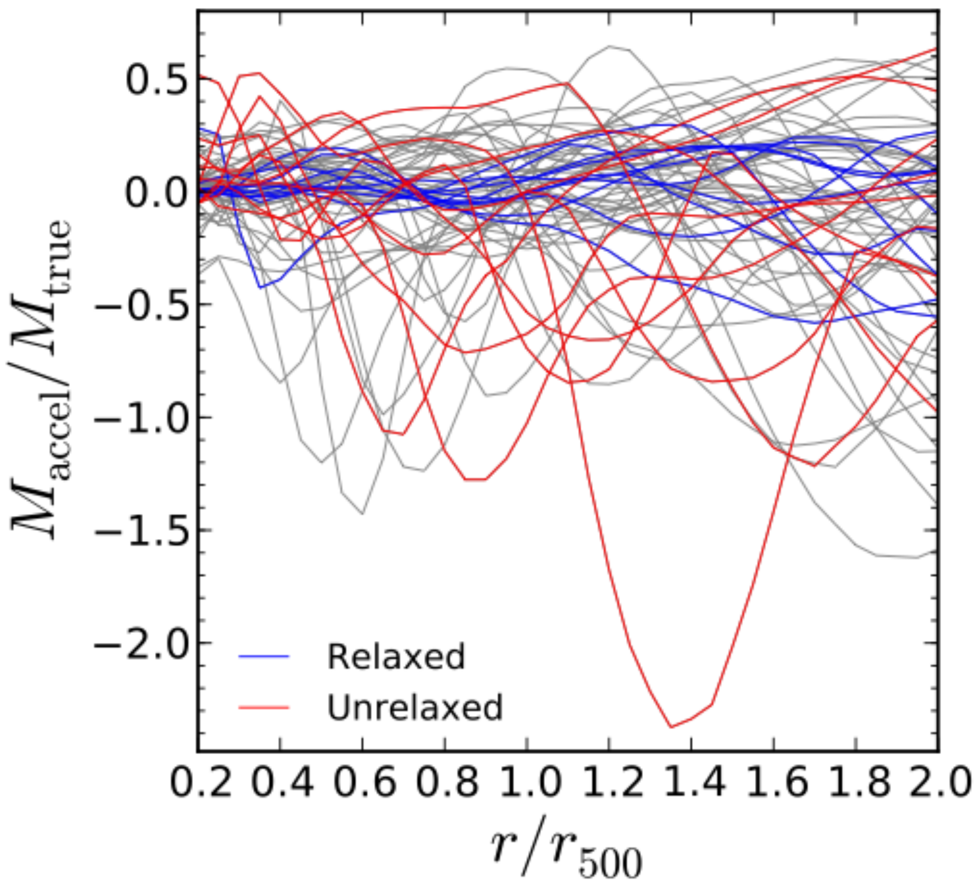

- Reduce bias and scatter for the full sample
- Scatter in relaxed clusters subsample reduced by half
- Unrelaxed systems still have significant mass bias (12%)

Gas acceleration introduces additional "irreducible" HSE mass bias

Nelson et al. 2014; see also Suto et al. 2013, Lau, Nagai, Nelson 2013

Measuring Gas Velocities and Non-thermal Pressure with ASTRO-H

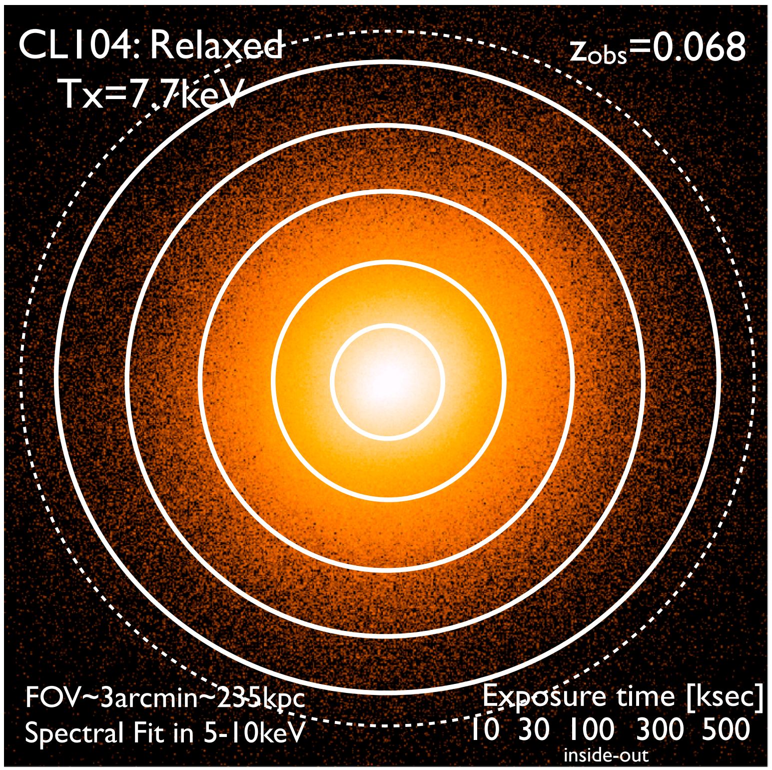

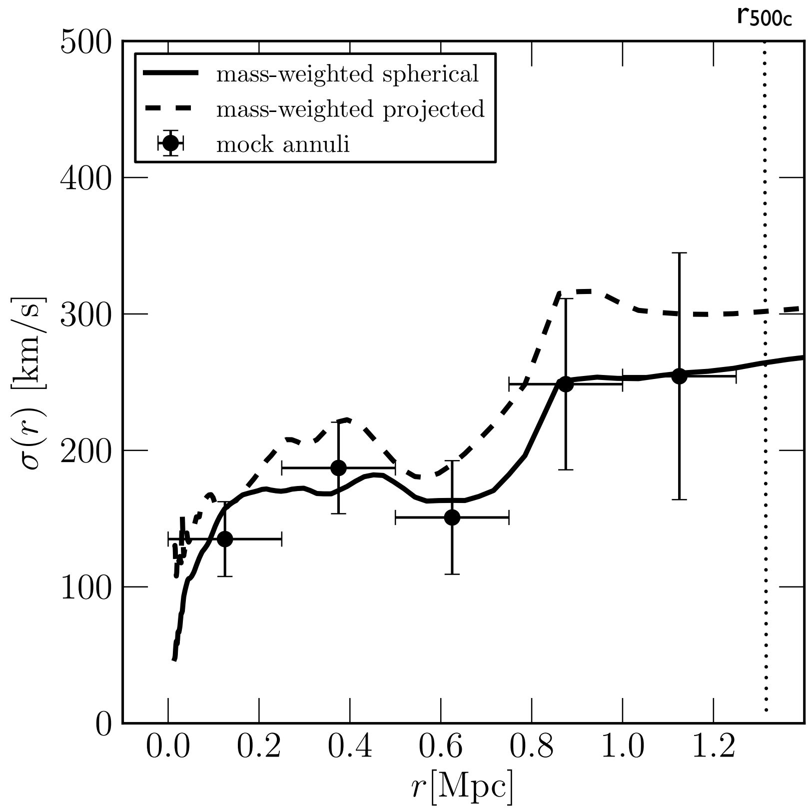

Mock ASTRO-H Simulation

X-ray spectroscopy can measures gas velocities along the line-of-sight through the Doppler broadening of Fe lines.

(Nagai, Lau, Avestruz, Nelson, Rudd, 2013, ApJ, 777, 137)

Measuring Gas Velocities and Non-thermal Pressure with Kinetic SZ Effect

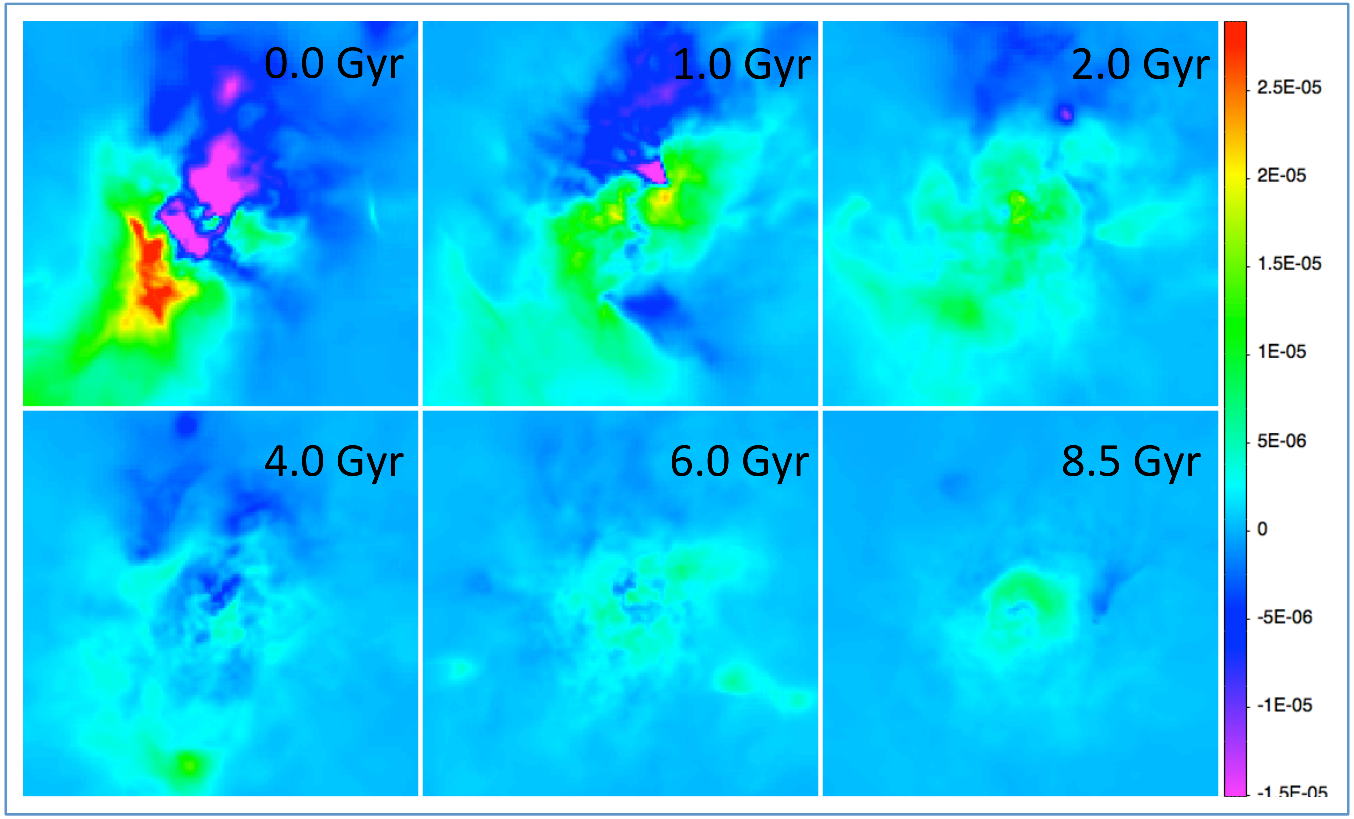

SZ effect is independent of redshift, making it ideal to measure the signal out to large radii and high-redshift. Kinematic SZ signal is sensitive to the internal gas motions in clusters.

Non-thermal Pressure Profile

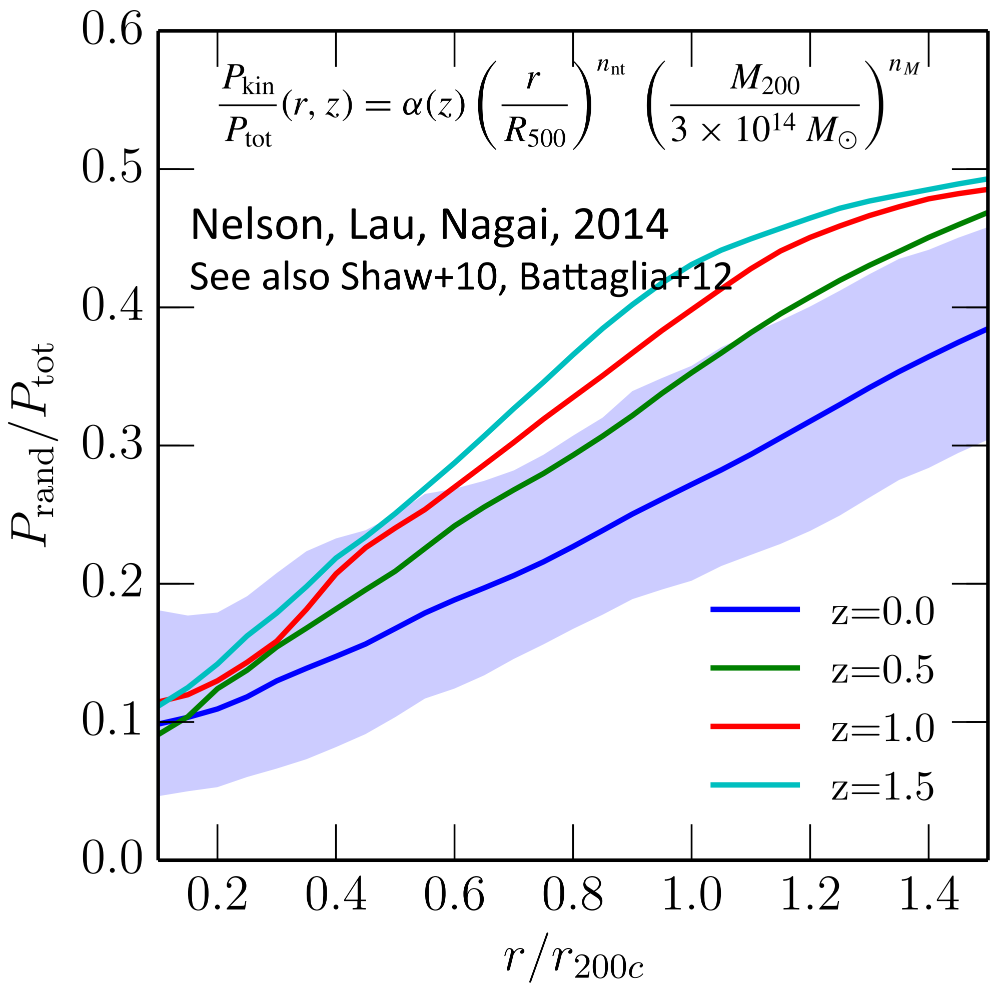

Strong redshift dependence:

Higher redshift clusters have higher non-thermal pressure?

Universal Non-thermal Pressure Profile

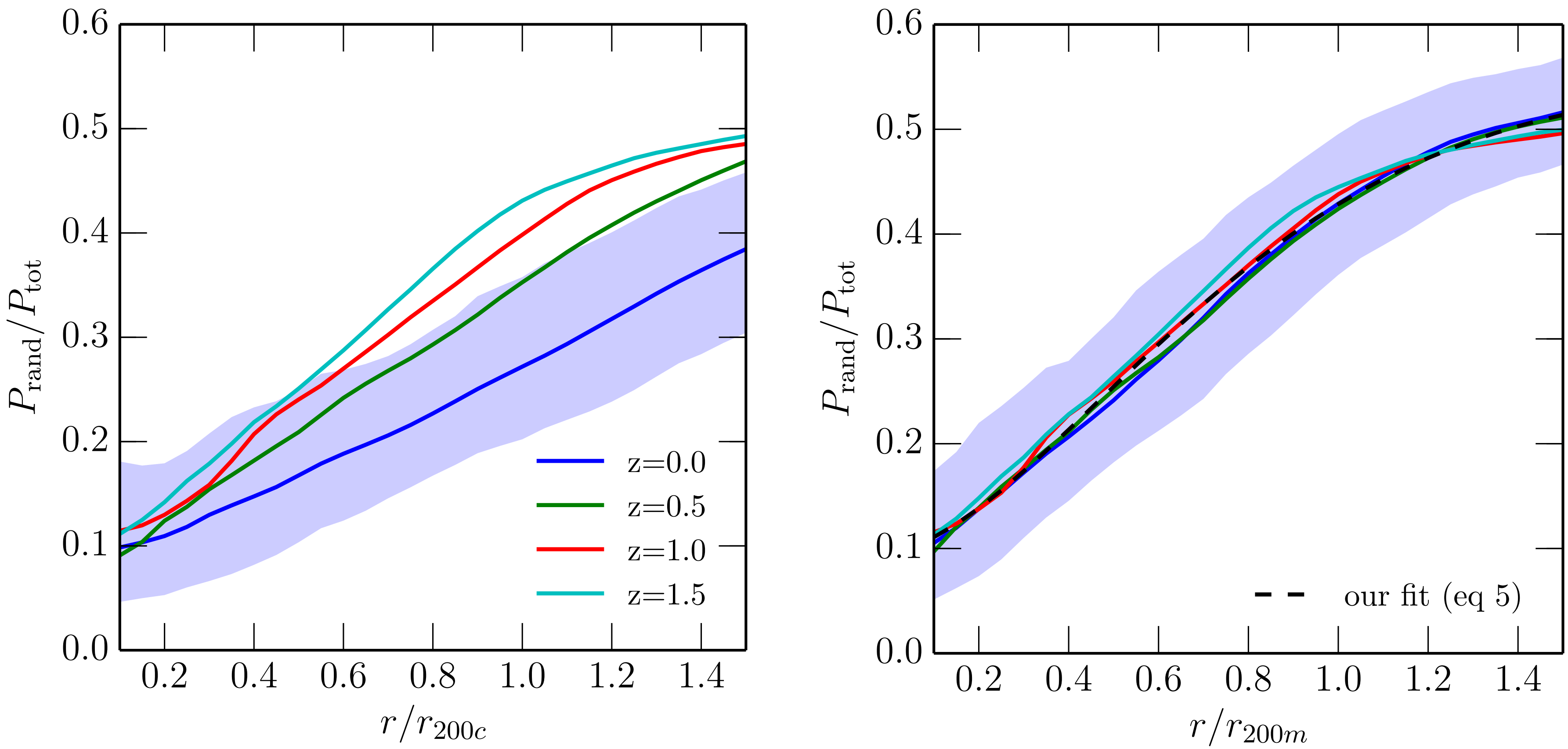

Non-thermal pressure fraction is "universal" when the profiles are normalized with respect to the "mean" density of the universe, instead of the "critical" density.

Origin of Scatter in the Non-thermal Pressure Profiles in Clusters

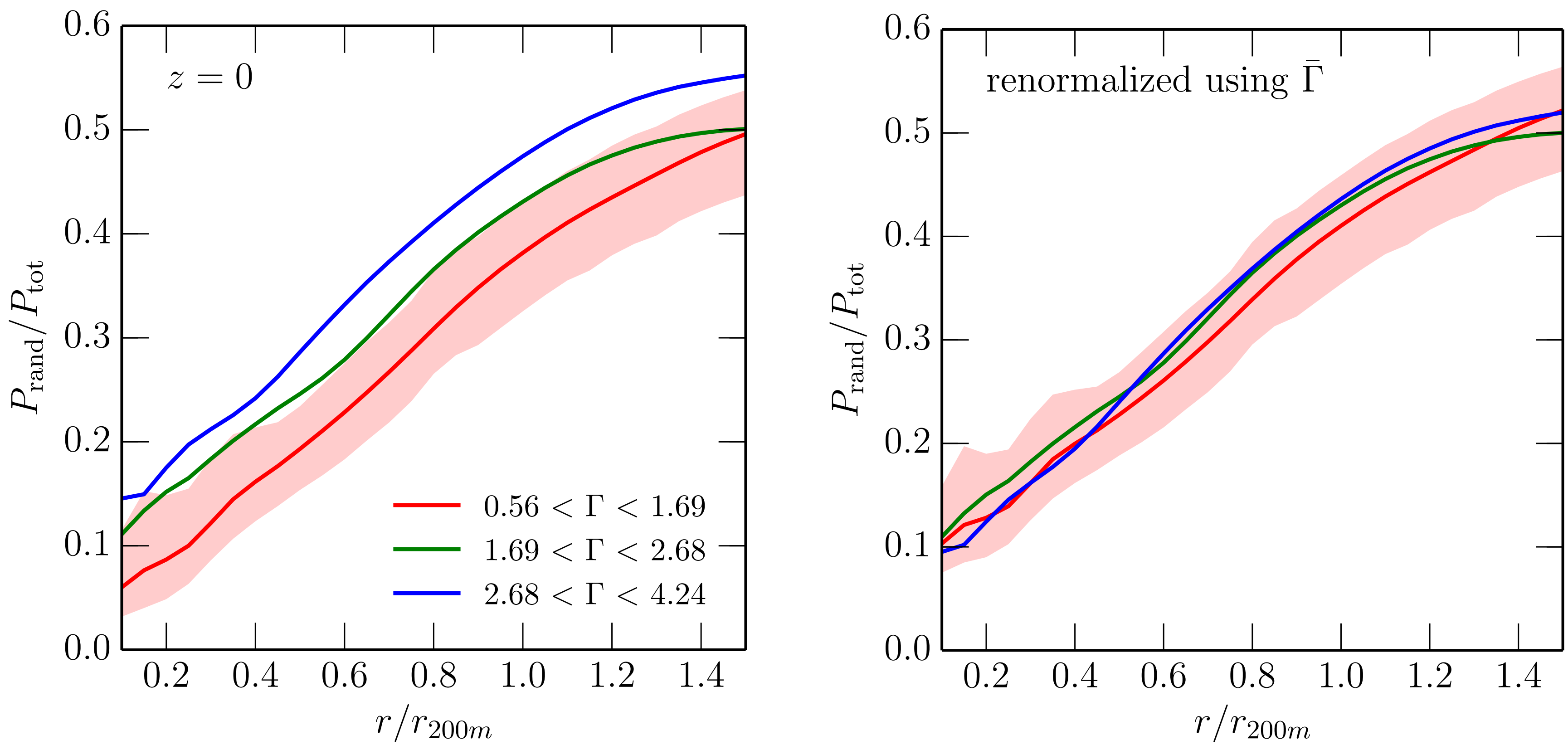

Strong dynamical state dependence. Important implications for the HSE mass bias as well as the SZ power spectrum measurements

Summary and Future Work

- New Omega 500 high resolution cluster sample
  - 65 simulated massive clusters from 500 Mpc/h box
- Cluster masses are biased by presence non-thermal pressure from gas motions (both velocities and accelerations) for all dynamical states
- Non-thermal pressure fraction is universal when defined with respect to the mean density of the universe

- Future Work: Dynamical state of a cluster has a significant effect on non-thermal pressure support and effects of different accretion modes need to be well quantified

Removal of Gas Inhomogeneities

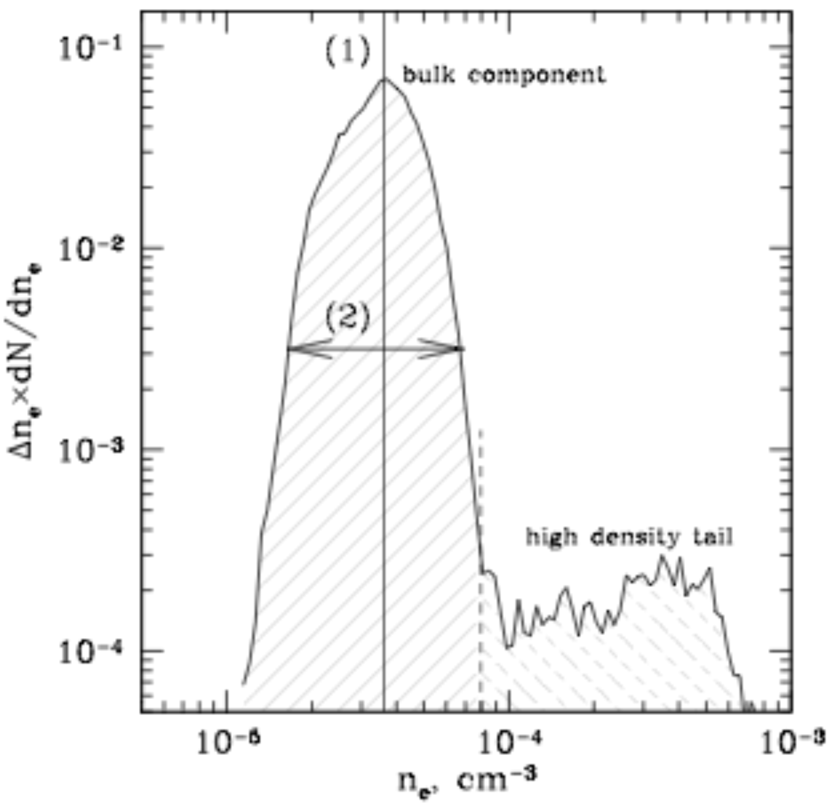

Gas “inhomogeneities” consist of (1) bulk component + (2) high density tail.

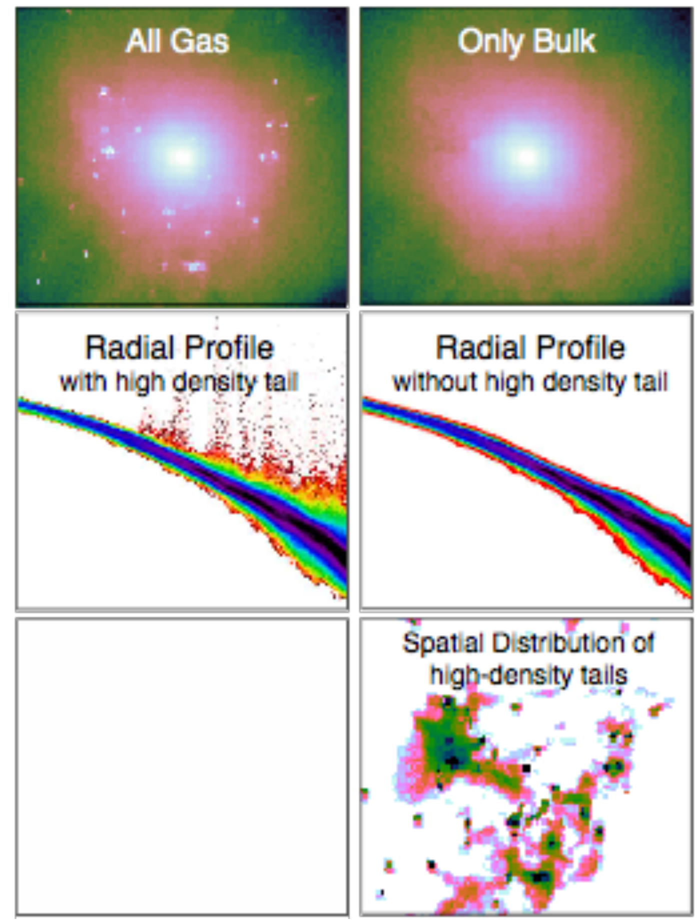

Zhuravleva et al. 2013;
see also Roncarelli+13, Vazza+13

Origin of Scatter in the Non-thermal Pressure Profiles in Clusters

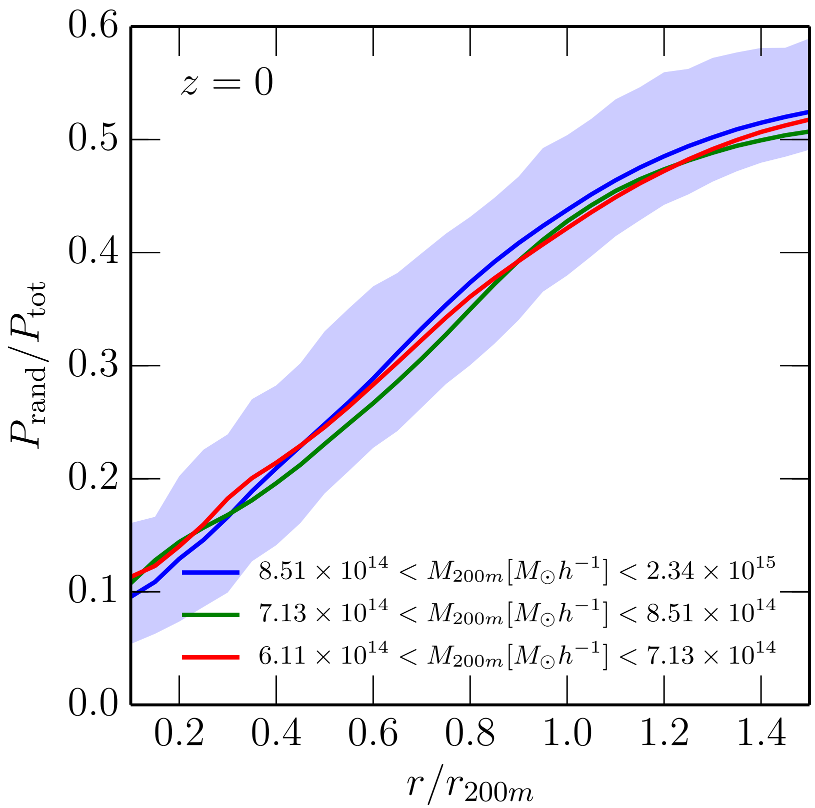

Little or no mass dependence.